Lower critical magnetic field of lithium containing $Bi_2Sr_2CaCu_2O_{8+\delta}$ single crystals

T. HORIUCHI, K. KITAHAMA*, T. KAWAI
The Institute of Scientific and Industrial Research, Osaka University,
8-1 Mihogaoka Ibaraki 567, Japan

Lower critical magnetic field strength at 0 K, $H_{c1}(T)$; $T = 0$ K, has been evaluated on single-crystal $Bi_{2.2}Sr_{1.8}Ca(Cu_{1-x}, Li_x)_2O_y$ with $0 \leqslant x \leqslant 0.13$ from d.c. susceptibility data. Significant change is noted between lithiuim-doped and undoped crystals: the value of $H_{c1}(0)$ decreases with increasing lithium content when the magnetic field is applied to the direction parallel to the *ab*-plane, i.e. the cleaved crystalline plane, while the value remains constant when the direction of the field is perpendicular to the *ab*-plane. This could be attributed to the change in penetration depth along the *c*-axis, i.e. λ_c, with lithium incorporation. Analyses of diamagnetism versus temperature data were made, which exhibited no significant change in electron-transport mechanism with the variation of lithium content.

1. Introduction

With the aim surveying and understanding the transport mechanism, of high T_c materials, substitution for copper with other metal ions has extensively been attempted in $Bi_2Sr_2CaCu_2O_{8+\delta}$ (Bi2212) [1–6]. Most of these trials, *e.g.* with one of iron, cobalt, nickel or zinc, resulted in lowering of T_c [1,2]. Elevation of T_c by lithium addition to the starting materials was found first by the authors [4]. Lithium substitution for copper in the crystal was supposed from a combined knowledge of the chemical analysis, observed density and preparation procedures [5]. However, no direct evidence of such replacement has yet been obtained. Moreover, the increment of T_c associated with lithium incorporation exceeds no more than 4 K despite the drastic modification of the CuO_2 layers in the structure, which play important roles in the conduction mechanism [3,6]. Studies so far made include syntheses of polycrystalline materials [3–5], preparation of single crystals [6], a Raman spectroscopic study [7] and measurements of electric conductivity and magnetic susceptibility [3–6]. At the present time, incorporation of lithium into the material has been found to induce only a small difference or almost no change in any physical properties.

Lower critical field at 0 K, $H_{c1}(0)$, as well as T_c has historically been an important physical quantity for the construction of the magnetic phase diagram. For example, the value at an arbitrary temperature, $H_{c1}(T)$ was predicted according to $H_{c1}(T) = H_{c1}(0)(1 - (T/T_c)^2)$ in the two-fluid model in 1934 [8]. For characterization of superconductive materials, $H_{c1}(0)$ is convenient, because it can be obtained rather easily at a magnetic field with only moderate strength. The purpose of the present work was to detect change in $H_{c1}(0)$ associated with lithium incorporation into the Bi2212 type superconductor. Changes in the conduction mechanism will also be examined by use of magnetic susceptibility, χ, versus. T data, taken at both low-field and mean-field conditions, and from the viewpoint of penetration length, λ. Throughout this paper, $H_{c1}(0)$ with the applied field parallel to the *ab*-plane (*i.e.* the morphology plane) and perpendicular to the *ab*-plane are expressed by $H_{c1}^{//ab}(0)$ and $H_{c1}^{\perp ab}(0)$, respectively. Penetration lengths associated with the shielding current J, in the *ab*-plane, $J_{//ab}$, and along the *c*-axis, $J_{\perp ab}$, are designated as λ_{ab} and λ_c, respectively.

2. Experimental procedure

Single crystals used in the present study were prepared by a travelling solvent floating zone (TSFZ) method, details of which are given elsewhere [6]. The chemical composition of each crystal was found from an inductively coupled plasma (ICP) analysis. The measurement of magnetization was performed on five crystals with formulas $Bi_{2.2}Sr_{1.8}Ca(Cu_{1-x}, Li_x)_2O_y$ ($x = 0$, 0.014, 0.030, 0.050 and 0.13), with the last one being the lithium solubility limit. A typical crystal used for the measurement weighed 1.3 mg and was in the shape of a flat plate with dimensions $2 \times 1 \times 0.1$ mm^3. For evaluation of magnetic susceptibility, the volume was calculated from sample weight and observed density.

The temperature dependence of magnetization, M, was observed in the range 4.2–100 K by both

---

*Author to whom all correspondence should be addressed.

zero-field cooling (ZFC) and field cooling (FC) conditions. In the former experiment, a crystal was cooled down to 4.2 K followed by application of a field and programme-controlled heating, while programme-cooling after application of the field at a temperature above T_c was used in the latter. Cooling was attained by exposing sample in a gelatin capsule to a stream of cold helium vapour. All magnetic measurements were made on a Hoxan HSM-2000 magnetometer equipped with a superconducting quantum interference device (SQUID). Field strengths are calibrated by use of powdered lead with high purity. Correction of demagnetization was made according to the formula

$$H = H_a/(1-\nu) \qquad (1)$$

where H_a and H represent applied and corrected fields, respectively. The coefficient ν was obtained from the initial slope of the M versus. H_a curve [9]. In the case of H_a perpendicular to the ab-plane, the value of ν ranged from 0.90–0.95, while smaller ν was observed ($\nu < 0.2$) when H_a was parallel to the ab-plane.

3. Results and discussion
3.1. Evaluation of $H_{c1}(0)$
The difficulty of precise determination of H_{c1} at low temperatures in isothermal measurements due to increase of super-current density was pointed out by Naito et al. [10,11]. They also proposed an excellent way to deduce H_{c1} from the measurement [10,11]. However, it appears sufficient to obtain crude $H_{c1}(0)$, because the aim of the present study was to detect whether any change exists between lithium-doped and undoped Bi2212 samples. Therefore, attention was paid to the change in χ versus. T behaviour with the change in field strength.

The temperature dependence of χ was measured on single crystals of $Bi_{2.2}Sr_{1.8}Ca(Cu_{1-x}, Li_x)_2O_y$ with $x = 0$–0.13, in which magnetic field was applied either parallel ($H_{//ab}$) or perpendicular ($H_{\perp ab}$) to the ab-plane. An example for the lithium composition $x = 0.05$ is shown in Fig.1, where several ZFC χ versus. T dependences are overlaid with field strengths, $H_{//ab} = 0.6$, 2.8 3.0 3.2 and 5.4 Oe. In this figure, χ keeps the theoretical constant value of $-1/4\pi$ (in c.g.s units) at low field strengths and in the low-temperature ranges due to perfect flux expulsion. However, it is also noted that χ–T dependencies bend upwards with increasing temperature after passing through an onset temperature, T_{ons}. This is the temperature above which magnetic fluxes begin to penetrate into the bulk. In other words, $H_{c1}(T_{ons})$, corresponds to the critical field strength at the temperature T_{ons}. The onset shifts towards the low temperature side and becomes round with increasing field strength. This roundness reflects the temperature dependence of the pinning force.

A similar evaluation of H_{c1} from temperature-dependent magnetization data was performed on Y–Ba–Cu–O by Krusin-Elbaum et al. [12] in which a point of intersection of initial slope in χ–T curve and abscissa, T_{c1}, was employed in place of our
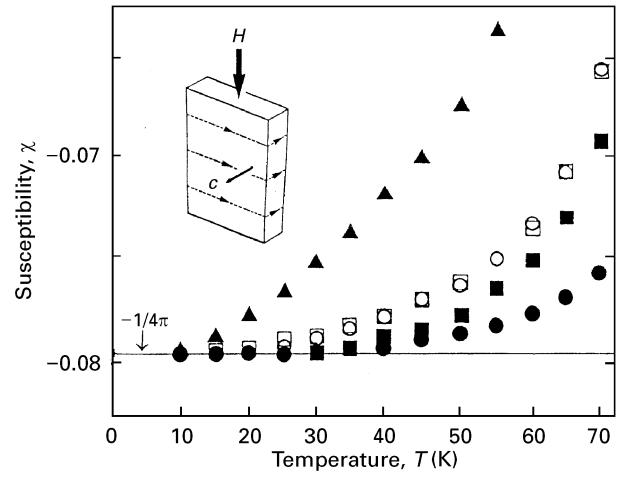
Figure 1 Temperature dependencies of magnetic susceptibility for $Bi_{2.2}Sr_{1.8}Ca(Cu_{1-x},Li_x)_2O_y$ ($x = 0.05$) with various magnetic field strengths parallel to the ab plane. (●) $H^{//ab} = 0.6$ Oe, (■) $H^{//ab} = 2.8$ Oe, (□) $H^{//ab} = 3.0$ Oe, (○) $H^{//ab} = 3.2$ Oe, (▲) $H^{//ab} = 5.4$ Oe. The direction of the field, that of the c-axis and a loop of the shielding current in a crystal are shown in the inset.

T_{ons}. In the present study, the value of T_{ons} was roughly estimated visually and plotted against H. Then it was extrapolated to the absolute zero temperature to obtain $H_{c1}(0)$. A tendency is also seen in Fig.1 that the radius of curvature at around T_{ons} increases with increasing field strength from 0 to $H_{c1}(0)$, while the curvature at 0 K begins to decrease with increasing H above $H_{c1}(0)$. This behaviour was also quite helpful in confirming that $H_{c1}(0)$ was reached when H was increased from below.

Fig. 2 summarizes the variation of $H_{c1}^{//ab}(0)$ and $H_{c1}^{\perp ab}(0)$ with lithium composition. Throughout the range within the solubility limit, $H_{c1}^{//ab}(0)$ exhibits a monotonic decrease with increase in lithium content while $H_{c1}^{\perp ab}(0)$ remains unchanged. This would arise from the difference in the direction of the shielding current. The closed circuit of the shielding current in $H_{c1}^{//ab}(0)$ consists of current both parallel, $J_{//ab}$, and perpendicular $J_{\perp ab}$ to the ab-plane, with the latter on the edge surface of the crystal. On the other hand, the shielding current in $H_{c1}^{\perp ab}(0)$ includes only $J_{//ab}$. On these grounds, it could be concluded that the dependence of $H_{c1}^{//ab}(0)$ on lithium composition may be attributed to the change in $J_{\perp ab}$ (and accordingly in λ_c) with lithium incorporation. More discussions on the lithium composition dependence will be given later.

Penetration depth and H_{c1} can be related roughly by

$$H_{c1} \approx \Phi_0/\pi\lambda^2 \qquad (2)$$

where Φ_0 is the flux quantum [13], which yielded $\lambda_{ab}(0) = 0.4$ μm for samples irrespective of lithium doping and $\lambda_c(0) = 1.5$ μm for the undoped crystal and $\lambda_c(0) = 2.1$ μm for $Bi_{2.2}Sr_{1.8}Ca(Cu_{1-x}, Li_x)_2O_y$ with $x = 0.13$. The values $\lambda_{ab}(0)$ of our observation are in good agreement with that (i.e. $\lambda_{ab}(0) = 500$ nm) reported by Maeda et al. [14]. On the other hand, $\lambda_c(0)$s for both doped and undoped materials are considerably lacking in comparison with the data
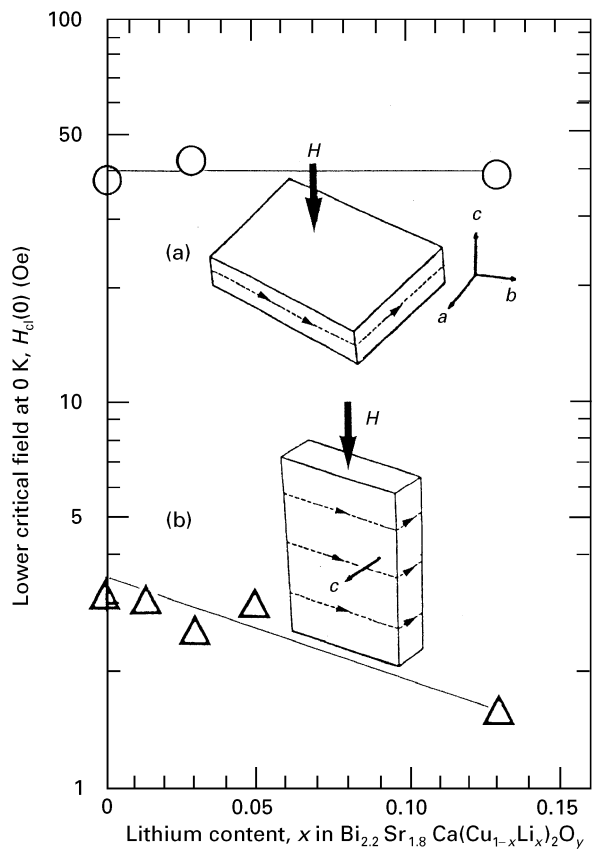
Figure 2 Dependence of $H_{c1}^{//ab}(0)$ and $H_{c1}^{\perp ab}(0)$ on lithium composition in $Bi_{2.2}Sr_{1.8}Ca(Cu_{1-x}Li_x)_2O_y$ with $x = 0$–0.13. (a) $H_{c1}^{\perp ab}(0)$. (b) $H_{c1}^{//ab}(0)$. Directions of the field, that of the c-axis and a loop of the shielding current in a crystal are indicated in each inset.

$[\lambda_c(0) = 100 \pm 10\ \mu m]$ measured on polycrystalline samples [15].

3.2. Analysis of χ versus T dependence
3.2.1. Mean-field magnetization measurement

Distinction of two models, i.e. the defect model and the BCS model, was performed on $Bi_{2.2}Sr_{1.8}Ca$ $(Cu_{1-x}Li_x)_2O_y$ with $x = 0.13$ using χ versus. T dependence measured in the range $H_{c1} \ll H \ll H_{c2}$ (the so-called mean field), where M versus. H is reversible. According to Hebard et al. [16], the dependence of $\lambda^{-1} \propto T_c - T$, is expected if the superconductivity is influenced by defects, while the relation of $\lambda^{-2} \propto T_c - T$, should be obeyed in the BCS behaviour. By using the relation of $dM/d(\ln H) \propto \lambda^{-2}$ proposed by Kogan et al. [17], $dM/d(\ln H) \propto (1 - T/T_c)^2$ and $dM/d(\ln H) \propto (1 - T/T_c)$ were found for the defects model and the BCS model, respectively.

Curves of ZFC and FC are shown in Fig. 3, as an example to demonstrate the reversible region above 80 K, which were measured at $H^{\perp ab} = 570$ Oe (after demagnetization correction). Fig. 4 compares the M versus In H plot at various temperatures near T_c. The slopes of $dM/d\ln H$ thus obtained were plotted again against $1 - T/T_c$ on a logarithmic scale, as shown in Fig. 5, which yielded the slope of -1, with the negative sign coming from diamagnetism. From this result, it is confirmed that the BCS behaviour
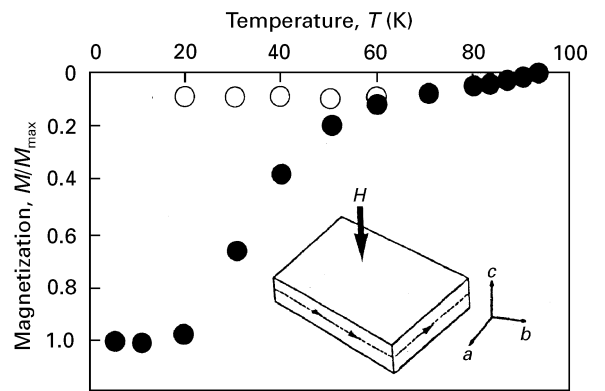

Figure 3 An example of the M versus T behaviour at $H^{\perp ab} = 570$ Oe (after correction of demagnetization) for $Bi_{2.2}Sr_{1.8}Ca(Cu_{1-x}Li_x)_2O_y$ with $x = 0.13$. A reversible region is noted above ~ 80 K. (●) ZFC, (○) FC.
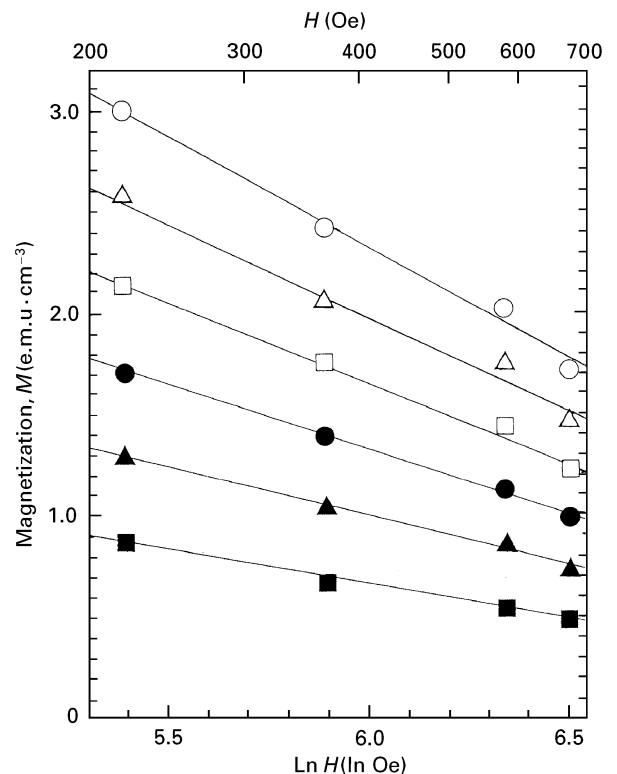

Figure 4 Plots of M versus ln $H^{\perp ab}$ in the reversible region to evaluate slopes of $dM/d(\ln H^{\perp ab})$ for $Bi_{2.2}Sr_{1.8}Ca(Cu_{1-x},Li_x)_2$-$O_y$ with $x = 0.13$. (○) 80 K, (△) 82 K, (□) 84 K, (●) 86 K, (▲) 88 K, (■) 90 K.

is obeyed at least in the temperature range near T_c. In case of the undoped Bi2212 sample, a behaviour of $\lambda^{-2} \propto T_c - T$ rather than $\lambda^{-1} \propto T_c - T$ near T_c, is reported [14]. Thus, it would be concluded that no change associated with lithium incorporation was detected with respect to the super-transport mechanism.

Throughout this section, we have dealt with data taken at the geometry $H^{\perp ab}$. Therefore, all of the above discussion is concerned only with $J_{//ab}$ and λ_{ab}.

3.2.2. Low-field magnetization measurement

The statement in Section 3.1 that χ remains constant at $-1/4\pi$ below T_{ons} is not exactly true.
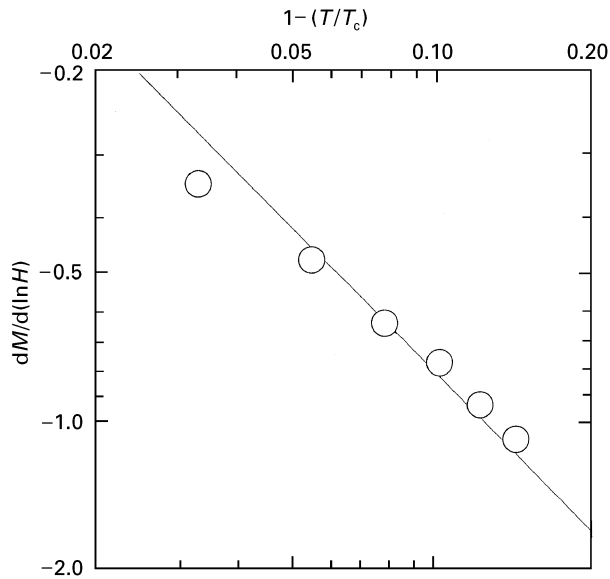
Figure 5 A plot of $dM/d(\ln H^{\perp ab})$ against $1 - (T/T_c)$.

Figure 6 Comparison of $\log(\Delta\chi/\chi(0))$ versus. $\log(T/T_c)$ plots at $H^{\parallel ab} = 0.8\,\mathrm{Oe}$ for lithium-doped and undoped crystals, $Bi_{2.2}Sr_{1.8}Ca(Cu_{1-x}, Li_x)_2O_y$ with $x = 0$ and 0.13. ($\bigcirc$) Undoped crystal, ($\bullet$) lithuim-doped crystal.

Fluxes penetrate into the skin of the sample with thickness λ, so that the value of χ is larger than $-1/4\pi$ by $\sim 0.1\%$, even at $0\,K$. This difference increases with increasing temperature and amounts to a few per cent at a temperature just below T_{ons}. Characterization of the lithium-containing crystal was also undertaken using the temperature dependence of $\Delta\chi$ ($= \chi(T) - \chi(0)$).

In this experiment, magnetic field was applied to the direction parallel to the *ab*-plane at $H^{\parallel ab} = 0.8\,\mathrm{Oe}$, the value being well below the $H_{c1}^{\parallel ab}(0)(= 1.6\,\mathrm{Oe})$. Designating $\lambda(T) - \lambda(0)$ as $\Delta\lambda(T)$, $\Delta\chi$ can be related to $\Delta\lambda$ according to

$$\Delta\chi(T)/\chi(0) = 2\Delta\lambda(T)/d \qquad (3)$$

where d is the sample thickness [18]. The temperature dependence of $\Delta\lambda$ was examined by plotting $\Delta\chi(T)/\chi(0)$ ($= 2\Delta\lambda(T)/d$) in the temperature range below $0.3T_c$ against T/T_c on a logarithmic scale for the $Bi_{2.2}Sr_{1.8}Ca(Cu_{1-x}, Li_x)_2O_y$ crystals with both $x = 0$ and 0.13, which are compared in Fig. 6.

A linear dependence with a slope of unity is yielded for both crystals. However, their intercepts with the ordinate differ due to the difference in sample thickness. Such a T dependence (other than T^2) of $\Delta\lambda$ can occur, for example, in a clean BCS-type *d*-wave superconductor with line nodes in the gap [19]. Crossover with the dependency $\Delta\lambda \propto T^2$ below $10\,K$ is reported in the crystal of $YBa_2Cu_3O_7$ doped with 0.15% Zn as an impurity [20]. Because no such tendency is perceived in the lithium doped crystal, the role of lithium as an impurity is not yet confirmed, although data points scatter considerably. To summarize, we could not detect any change associated with lithium incorporation into the material in the $\Delta\lambda$ versus. T behaviour also in the low-temperature range.

3.3. Dependence of $H_{c1}^{\parallel ab}(0)$ on lithium composition

As described in Section 3.1, it was revealed that $H_{c1}^{\parallel ab}(0)$ depends on lithium composition, which is
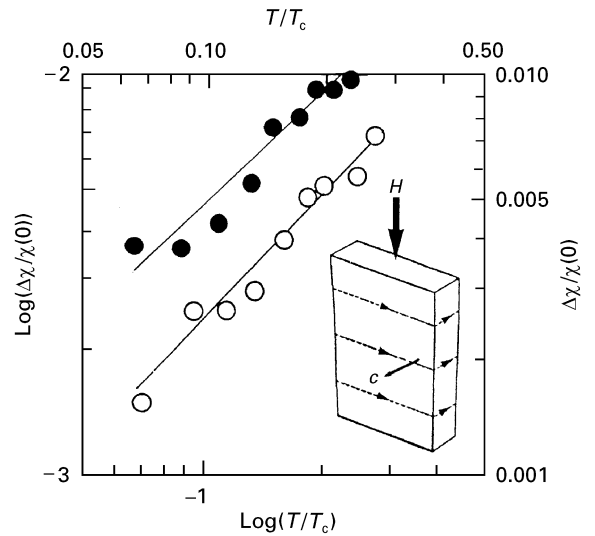
attributable to the change in $J_{\perp ab}$ (or λ_c) with lithium incorporation into the crystal. As sources of this dependence, the following two origins are postulated. One is the change in lattice parameter along the *c*-axis. The structure consists of alternation of a conductive CuO_2 double layer (*i.e.* CuO_2–Ca–CuO_2) and an insulating $Bi_2Sr_2O_4$ layer. Small but significant elongation of the *c* axis is observed [5], so that interaction between neighbouring CuO_2 layers may be reduced. However, this change does not appear to be sufficient for the explanation, because the difference in the length of the *c* axis is quite small.

The other cause would be the change in carrier density associated with lithium incorporation into the crystal. For simplicity, substitution by Li^+ for some divalent ion might increase hole concentration, if the number of oxygens in the crystal does not change. On the other hand, lowering of the formation temperature by less than $50\,K$ associated with lithium incorporation is observed in the experiment of the crystal growth [6], which increases oxygen content in the material and finally results in a small increase in T_c [3–6]. Such a change in carrier concentration indirectly influences the electron transport mechanism along the *c*-axis and might eventually decrease $J_{\perp ab}$.

4. Conclusion

By using single crystals, a comparison of χ versus T behaviour has been made between a lithuim-doped and an undoped oxide superconductor of the type $Bi_2Sr_2CaCu_2O_{8+\delta}$ Significant change was noted in $H_{c1}^{\parallel ab}(0)$, which decreases with increasing lithium content, while $H_{c1}^{\perp ab}(0)$ remains unchanged. It is evident that the former difference arises from the change in $J_{\perp ab}$ (or λ_c). Although the reason for this remains unclear, change in oxygen content appears to be responsible, rather than change in the length of the *c*-axis. No change in electron transport mechanism

associated with lithium incorporation was evinced from the present analysis of the χ versus T data.

References

1. T. KANAI, T. KAMO and S. MATSUDA, *Jpn J. Appl. Phys.* **28** (1989) L551.
2. A. MAEDA, T. YABE, S. TAKEBAYASHI, M. HASE and K. UCHINOKURA, *Phys. Rev.* **B41** (1990) 4112.
3. S. X. DOU, H. K. LIU, W. M. WU, W. X. WANG and C. C. SORRELL, *Physica C* **172** (1990) 295.
4. T. KAWAI, T. HORIUCHI, K. MITSUI, K. OGURA, S. TAKAGI and S. KAWAI, *ibid.* C **161** (1989) 561.
5. T. HORIUCHI, T. KAWAI, K. MITSUI, K. OGURA and S. KAWAI, *ibid.* **168** (1990) 309.
6. T. HORIUCHI, K.KITAHAMA and T.KAWAI, *ibid.* **221** (1994) 143.
7. P.V. HUONG, H. WANG, K. KITAHAMA, T. HORIUCHI and T. KAWAI, Abstract of MRS Fall Meeting, Boston, President J. C. Bravmann (Materials Research Society, 1994) p. 322, H23. 26.
8. C. J. GORTER and H. B. G. CASIMIR, *Physik Z.*, **35** (1934) 963.
9. A. UMEZAWA, G. W. CRABTREE, J. Z. LIU, T. J. MOREN, S. K. MALIK, L. H. NUNEZ, W. L. KWOK and C. H. SOWERS, *Phys. Rev.* **B38** (1988) 2843.
10. M. NAITO, S. KAMBE and K. KITAZAWA, *Kotai Butsuri* **26** (1990) 23.
11. M. NAITO, A. MATSUDA, K. KITAZAWA, S. KAMBE, I. TANAKA and H. KOJIMA, *Phys. Rev* . **B41** (1990) 4823.
12. L. KRUSIN-ELBAUM, A. P. MALOZEMOFF, Y. YESHURUN, D. C. CRONEMEYER, and F. HOLTZBERG, *ibid.*, **B39** (1989) 2936.
13. C. KITTEL, "Introduction to Solid State Physics", 6th Ed (Wiley, New York, 1986). p. 236.
14. A. MAEDA, T. SHIBAUCHI, N. KONDO, K. UCHINOKURA, and M. KOBAYASHI, *Phys. Rev.* **B46** (1992) 14234.
15. J.R. COOPER, L. FORRO and B. KESZEI, *Nature* **343** (1990) 444.
16. A. F. HEBARD, A. T. FIORY, M. P. SIEGAL, J.M. PHILIPS and R. C. HADDON, *Phys. Rev.* **B44** (1991) 9753
17. V. G. KOGAN, M. M. FANG and S. MITRA, *ibid.* **B38**, (1988) 11958.
18. L. KRUSIN-ELBAUM, R. L. GREENE, F. HOLTZBERG, A. P. MALOZEMOFF and Y. YESHURUN, *Phys. Rev. Lett.* **62** (1989) 217.
19. W. N. HARDY, D. A. BONN, D. C. MORGAN, R. LIANG and K. ZANG, *ibid.* **70** (1993) 3999.
20. D. ACHKIR, M. POIRIER, D. A. BONN, R. LIANG, and W. N. HARDY, *Phy. Rev.* **B48** (1993) 13184.